Evolution of Breaking Directional Spectral Waves in the Nearshore Zone

H. Tuba Özkan and James T. Kirby, M. ASCE [1]

Abstract

Methods used in parabolic refraction-diffraction models for computing the evolution of monochromatic waves in the nearshore zone are used to construct a model for spectral wave conditions. The two dimensional spectrum is divided into discrete wave components and the individual wave components are computed simultaneously in the domain using parabolic models for each wave component. Statistical quantities are computed at each forward step in the parabolic scheme and used to construct a statistical wave breaking model. The breaking model is built into the parabolic model equation using an additional breaking term. Model results are compared to available one- or two-dimensional data.

Introduction

The parabolic approximation has been shown to be a robust method for computing the evolution of monochromatic water waves in the nearshore zone (Kirby and Dalrymple, 1984). Recently, methods for computing a directional spectral sea state using the parabolic approximation have been developed. Panchang, et. al. (1990) and Grassa (1990) have each developed models which operate by first discretizing the spectrum into individual monochromatic directional components, and then running each component in a separate parabolic model. Results from the sequential runs are superimposed in order to obtain estimates of statistical wave heights. O'Reilly and Guza (1991) have further extended this formulation and have pointed out that the model could be used (in linear form) to develop a transfer function between onshore and offshore, after which any incident spectrum could be simply transformed using the computed transfer function.

In the nearshore region and especially near inlets, waves become strongly modified by significant variations in bathymetry and ambient current fields. These modifications lead, in turn, to depth-limited and current-limited breaking, which cause significant energy losses in the incident wave field and which are accompanied by strong nonlinear modifications of the wave field. In the models mentioned above, the assumptions made in model development or operation preclude an ability to predict local depth-limited breaking. The purpose of this study is to alleviate these restrictions and provide a platform for predicting strong breaking

[1]Center for Applied Coastal Research, Department of Civil Engineering, University of Delaware, Newark, DE 19716

energy losses in directional spectral seas in the vicinity of tidal inlets.

Description of the Modeling Scheme

The parabolic model for spectral wave conditions used here requires the input of a directional random sea at the offshore boundary. The random sea is represented by a two-dimensional spectrum in frequency and direction and is discretized resulting in wave components. The evolution of these wave components is computed simultaneously at each forward step in the parabolic scheme. Therefore, after each forward step in the shore normal direction it is possible to determine statistical properties on that row before taking another step forward. These statistical quantities are incorporated into a statistical wave breaking model.

In the following sections the wave field resulting from the discretization is described, the model equation for the individual wave components is stated and the incorporation of the breaking model is explained. Furthermore, an initial attempt to include significant effects of nonlinearity on the wave field is described.

Wave Climate

The discretization process of the two dimensional spectrum results in wave components of amplitude A with an associated frequency f and an angle of incidence θ to the assumed propagation direction. The water surface elevation can be described in terms of these discrete wave components. It is assumed that the water surface elevation η is periodic in time and that the spatial dependency can be split into a fast-varying phase and a slow-varying amplitude.

$$\eta(x,y,t) = \sum_{allf}\sum_{all\theta}\left\{\frac{A(x,y;f,\theta)}{2}e^{i\psi} + c.c.\right\} \tag{1}$$

where f is the frequency, θ is the direction of any individual wave component and

$$\psi = \int \mathbf{k}\cdot d\mathbf{x} - \omega t \tag{2}$$

In order to determine energy losses associated with randomly occuring wave breaking, it is necessary to have estimates of the statistical wave height at each point in the model grid as computation passes that point. Using the computed information about the spectral components at a location (x,y) the significant wave height can be computed as

$$H_{1/3}(x,y) = \sqrt{8\sum_{n=1}^{N}|A(x,y)_n|^2} \tag{3}$$

where N is the total number of wave components and $A(x,y)_n$ is the amplitude of the wave component n at location (x,y).

Wave Models for Individual Wave Components

The refraction, diffraction and shoaling of the discrete wave components is assumed to be governed by the parabolic approximation to the mild slope equation derived by Berkhoff (1972). To minimize the restrictions placed on the range of allowed wave angles with respect to the assumed wave direction, the procedure derived by Booij (1981) is used, enabling the model to handle wave direction up

to about 45° from the shore normal, herein called x-direction. The model also has the ability to handle strong currents by using the formulation of the mild slope equation including the influence of currents derived by Kirby (1986).

The model uses the parabolic approximation including wave-current interactions and rederived for a wide angle approximation. The governing equation is:

$$
\begin{aligned}
& (C_{gn}+U)(A_n)_x - 2\Delta_1 V(A_n)_y + i(\bar{k}_n - a_0 k_n)(C_{gn}+U)A_n \\
+ & \left\{\frac{\sigma_n}{2}\left(\frac{C_{gn}+U}{\sigma_n}\right)_x - \Delta_1\sigma_n\left(\frac{V}{\sigma_n}\right)_y\right\}A_n + i\Delta_n'\left[\left((CC_g)_n - V^2\right)\left(\frac{A_n}{\sigma_n}\right)_y\right]_y \\
- & \; i\Delta_1\left\{\left[UV\left(\frac{A_n}{\sigma_n}\right)_y\right]_x + \left[UV\left(\frac{A_n}{\sigma_n}\right)_x\right]_y\right\} + \alpha A_n \\
+ & \frac{-b_1}{k_n}\left\{\left[\left((CC_g)_n - V^2\right)\left(\frac{A_n}{\sigma_n}\right)_y\right]_{yx} + 2i\left(\sigma_n V\left(\frac{A_n}{\sigma_n}\right)_y\right)_x\right\} \\
+ & \; b_1\beta_n\left\{2i\omega_n U\left(\frac{A_n}{\sigma_n}\right)_x + 2i\sigma_n V\left(\frac{A_n}{\sigma_n}\right)_y - 2UV\left(\frac{A_n}{\sigma_n}\right)_{xy}\right. \\
+ & \left.\left[\left((CC_g)_n - V^2\right)\left(\frac{A_n}{\sigma_n}\right)_y\right]_y\right\} - \frac{i}{k_n}b_1\left\{(\omega_n V)_y + 3(\omega_n U)_x\right\}\left(\frac{A_n}{\sigma_n}\right)_x \\
- & \; \Delta_2\left\{\omega_n U\left(\frac{A_n}{\sigma_n}\right)_x + \frac{1}{2}\omega_n U_x\left(\frac{A_n}{\sigma_n}\right)\right\} + ik\omega_n U(a_0-1)\left(\frac{A_n}{\sigma_n}\right) = 0
\end{aligned}
\tag{4}
$$

where

$$
\begin{aligned}
\sigma_n &= \omega_n - k_n U \\
\beta_n &= \frac{(k_n)_x}{k_n^2} + \frac{\left(k_n\left((CC_g)_n - U^2\right)\right)_x}{2k_n^2\left((CC_g)_n - U^2\right)} \\
\Delta_1 &= a_1 - b_1 \\
\Delta_2 &= 1 + 2a_1 - 2b_1 \\
\Delta_n' &= a_1 - b_1\frac{\bar{k}_n}{k_n}
\end{aligned}
\tag{5}
$$

The model coefficients

$$
\begin{aligned}
a_0 &= 1 \\
a_1 &= -0.75 \\
b_1 &= -0.25
\end{aligned}
\tag{6}
$$

recover the approximation of Booij.

For more detailed information about the development of the wave model, the reader is referred to the documentation of the numerical model **REF/DIF S** by Kirby and Özkan (1992).

Özkan

The Breaking Model

The statistical information obtained after each step in the parabolic scheme is used to construct a model for the dissipation of energy due to breaking. The wave breaking scheme involves a uniform dissipation of energy over the individual wave components. The amount of total energy dissipation is a function of the local statistical quantities and the local water depth. Therefore breaking of individual waves in a wave train is not considered, but a spectral approach to the wave breaking process is taken.

To determine the uniformly distributed energy dissipation, a simple model by Thornton and Guza (1980) is used. They showed that the energy dissipation can be expressed as

$$\frac{\partial EC_g}{\partial x} = -\epsilon_b \tag{7}$$

where the energy E and the bore dissipation ϵ_b can be expressed as

$$E = \frac{1}{8}\rho g H_{rms}^2 \tag{8}$$

$$\epsilon_b = \frac{3\sqrt{\pi}}{16}\frac{\rho g \bar{f} B^3}{\gamma^4 h^5} H_{rms}^7 \tag{9}$$

Here h is the local water depth and $\bar{f}$ is a representative frequency for the frequency spectrum and is chosen to the peak frequency. Following Mase and Kirby (1992), the constants B and γ are chosen to be equal to 1 and 0.6, respectively. The root-mean-square (rms) waveheight can be written as

$$H_{rms} = \frac{1}{\sqrt{2}} H_{1/3} \tag{10}$$

The energy dissipation model is built into the model equation using an additional breaking term. The model equation includes terms that can easily be related to the energy flux EC_g. In the same manner the new dissipation term will be related to the bore dissipation ϵ_b. Therefore the model equation includes terms like

$$C_g \frac{\partial A}{\partial x} = -\alpha A \tag{11}$$

The coefficient α is given by

$$\alpha = \frac{4\epsilon_b}{\rho g H_{rms}^2} = \frac{3\sqrt{\pi}}{4}\frac{\bar{f} B^3}{\gamma^4 h^5} H_{rms}^5 \tag{12}$$

The magnitude of the coefficient α will be infinitesimally small when breaking does not occur but grows to a significant value when breaking starts to occur. Furthermore, the presence of the breaking term in the equation at all times makes any criterion for turning breaking on or off unnecessary. It should be noted, though, that no modifications have been made to Thornton and Guza's dissipation model to account for directional effects.

Nonlinear Formulation for the Wave Speed

It is anticipated that nonlinear effects, present during wave breaking, will cause the phase speed of the shoaling and breaking waves to increase with respect to the unbroken waves in the domain. An effect like this would cause waves on top of a submerged shoal to speed up with respect to the waves at the sides of the shoal, acting to nullify any focusing tendency. Because this would change the spatial wave field significantly, an initial attempt has been made to take the effect of the nonlinearity on the wave speed into account. It should be noted that the construction of a full nonlinear model to simulate this or other nonlinear effects is not within the scope of this study.

Hedges (1976) developed an approximate relationship for nonlinear dispersion of monochromatic waves in shallow water. This formulation involved a simple modification to the linear dispersion relation to approximate nonlinear behavior. The modified dispersion relation by Hedges (1976) is given by

$$\sigma^2 = gk \tanh\left(kh(1 + |A|/h)\right) \tag{13}$$

This formulation can be altered by using the significant wave height instead of the wave amplitudes in shallow water in an attempt to include the effect of a random sea. The Hedges (1976) formulation would then be altered to

$$\sigma^2 = gk \tanh\left(kh(1 + H_{1/3}/2h)\right) \tag{14}$$

It should be noted that in shallow water and for small $|A|/h$, the Hedges (1976) relationship represents the propagation speed of a solitary wave.

$$C^2 = gh\left(1 + |A|/h\right) \tag{15}$$

It can be argued that a breaking wave propagates with the speed of a bore which would be given by

$$C^2 = gh\left(1 + 3|A|/h\right) \tag{16}$$

which is larger than the shallow water relationship given by Hedges (1976). The application of this relationship to the model would cause the breaking waves in the domain to travel faster.

Comparison to Data

Five example cases will be discussed making use of experimental data collected by Vincent and Briggs (1989) and by Mase and Kirby (1992).The test set-ups for both experiments will be summarized and results presented and dicussed in the following sections.

Waves Shoaling on a Plane Beach

Mase and Kirby (1992) conducted experiments using a Pierson-Moskowitz spectrum without directional spreading. The waves were generated in constant depth of 47 cm, and then shoaled and dissipated on a 1 : 20 beach. Wave gages were placed at several locations on the beach. Figure 1 shows the set-up of the experiment in a wave flume.

The comparisons between this data set and the model will be made using Case 1 in Mase and Kirby (1992). The available data are in terms of time series at the wave gage locations. The time series are used to compute the significant wave

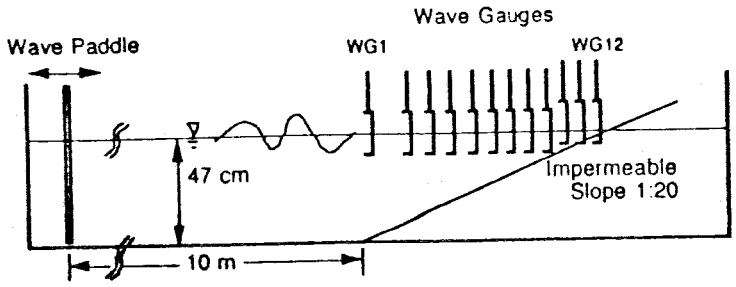

Figure 1: Experimental Setup (from Mase and Kirby (1992))

height for comparison with model results. Measured data at the offshore gage is used to create a smoothed incident frequency spectrum for the model input. The incident spectrum is divided into 50 discrete wave components. Figure 2 shows the incident frequency spectrum.

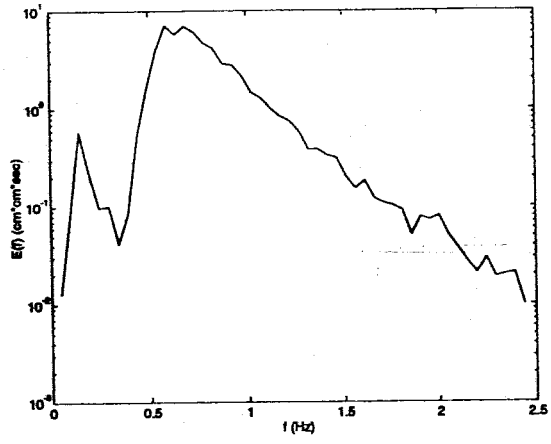

Figure 2: Incident Frequency spectrum

Results for this case are presented in Figure 3. It can be seen that the model shoals the waves up to the well predicted breaking point. The wave height decay after breaking starts is also very well predicted. The data points close to the shore show the presence of setup which the model cannot predict.

Waves over a Submerged Shoal

Vincent and Briggs (1989) conducted their experiments in a wave tank that is 35 m (114 ft) wide and 29 m (96 ft) long. The waves were generated by the directional spectral wave generator, which is 27.43 m (90 ft) long. The center of the shoal was located at $x = 6.10$ m and $y = 13.72$ m. The elliptical shoal had a major radius of $3.96m$, a minor radius of 3.05 m and a maximum height of 30.48 cm at the center. Maximum water depth was 47 cm. Expressions for the shoal perimeter and the elevation of each point on the shoal are given by Vincent and

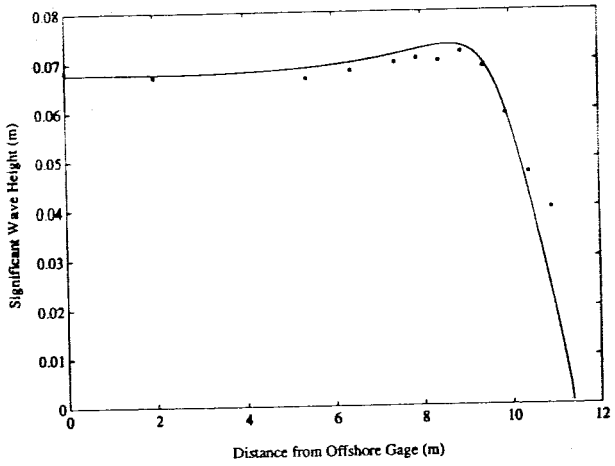

Figure 3: Waves Shoaling on a Beach: Significant Wave Height for Data and Model

Briggs (1989). Reference should be made to that document for further information about the domain.

Figure 4 shows the experimental set-up in the basin and the measurement transects 1–9. Data collection for the cases of interest to this study were only performed on transect 4.

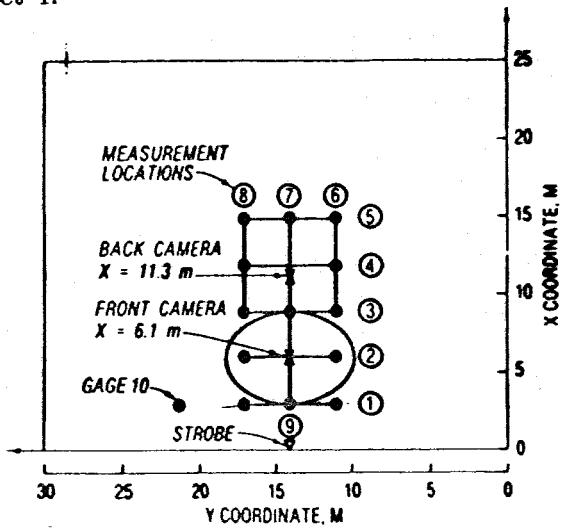

Figure 4: Experimental Setup (from Vincent and Briggs (1989))

In all the cases a TMA spectrum (Hughes, 1984) in conjunction with a directional spreading function was used to establish the target spectrum.

The TMA spectrum is given by the energy density $E(f)$ for frequency f

$$E(f) = \frac{\alpha g^2}{(2\pi)^4 f^5} \exp\left\{-1.25\left(\frac{f_m}{f}\right)^4 + (\ln\gamma)\exp\left[\frac{-(f-f_m)^2}{2\sigma^2 f_m^2}\right]\right\}\phi(f,h) \quad (17)$$

Özkan

where α is the Phillips' constant, f_m is the peak frequency and γ is the peak enhancement factor. Furthermore σ = shape parameter defined by

$$\sigma = \begin{cases} \sigma_a = 0.07 & \text{if } f < f_m \\ \sigma_b = 0.09 & \text{if } f \geq f_m \end{cases} \tag{18}$$

The factor $\phi(f,h)$ incorporates the effect of the depth h and is computed following Hughes (1984) by

$$\phi = \begin{cases} 0.5\,(\omega_h)^2 & \text{if } \omega_h < 1 \\ 1 - 0.5\,(2-\omega_h)^2 & \text{if } 1 \leq \omega_h \leq 2 \\ 1 & \text{if } \omega_h > 2 \end{cases} \tag{19}$$

where

$$\omega_h = 2\pi f \sqrt{\frac{h}{g}}$$

Narrow or broad frequency spectra used in the experiment can be obtained assigning the values 20 and 2 to the parameter γ, respectively. Representative plots of the narrow and broad frequency spectra are given in Figure 5.

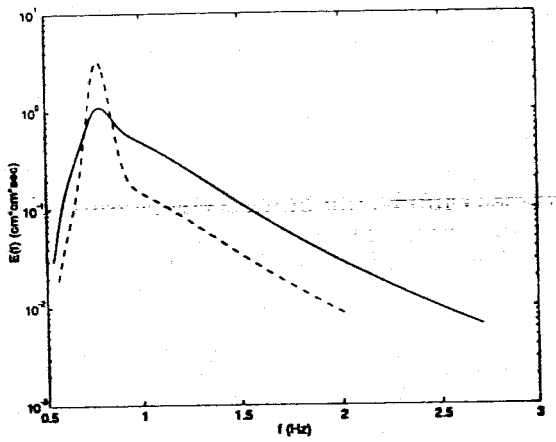

Figure 5: Narrow and Broad Frequency Spectra for $\alpha = 0.00047$

The directional spreading function (Borgman, 1985)is given by

$$D(\theta) = \frac{1}{2\pi} + \frac{1}{\pi}\sum_{j=1}^{J} \exp\left[-\frac{(j\sigma_m)^2}{2}\right] \cos j\,(\theta - \theta_m) \tag{20}$$

where

θ_m = mean wave direction = 0°.

J = number of terms in the series (chosen to be 20 in the numerical calculations).

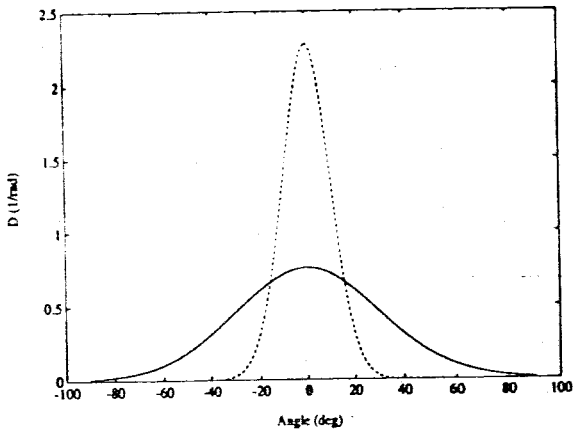

Figure 6: Narrow and Broad Directional Spreading Functions

σ_m is chosen to be 10° or 30° giving a narrow or broad directional spreading, respectively. Representative plots of the narrow and broad directional spreading functions are given in Figure 6.

The two-dimensional spectrum is then given by the product

$$S(f,\theta) = E(f)\,D(\theta) \tag{21}$$

For the simulation of these experiments, the target spectrum was divided into 10 frequency components and 20 directional components, yielding a total of 200 discrete wave components. Four cases out of this data set will be used for comparisons with the model. The first two cases do not involve breaking waves, whereas the next two cases involve intensive breaking of the waves over the submerged shoal.

Non-Breaking Cases

The first case is denoted as Case N4 by Vincent and Briggs (1989) and involves a narrow frequency spectrum used in conjunction with a narrow directional spreading. Another case (B4) involves a narrow frequency spectrum and a broad directional spreading. Neither of these cases involve breaking waves and are simulated to show that the breaking term that is always in effect does not induce an unrealistic wave height reduction.

Results for Case N4 are presented in Figures 7 and 8, where the first of these shows a contour plot of the computed normalized significant wave height and the second shows a comparison of model and data at Transect 4.

It can be seen that the general shape of the curve is well modeled. The fact that the peak of the wave height for this case with no wave breaking is well represented shows that the coefficient of the breaking term stays small and does not dissipate energy from the system.

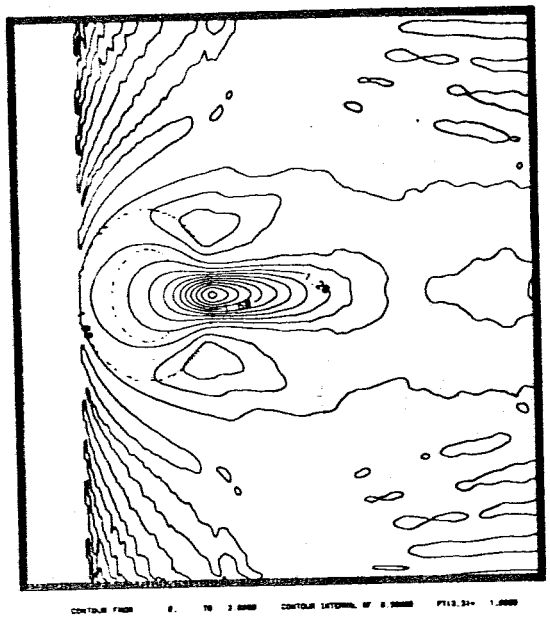

Figure 7: Case N4: Contour Plot of Normalized Significant Wave Height

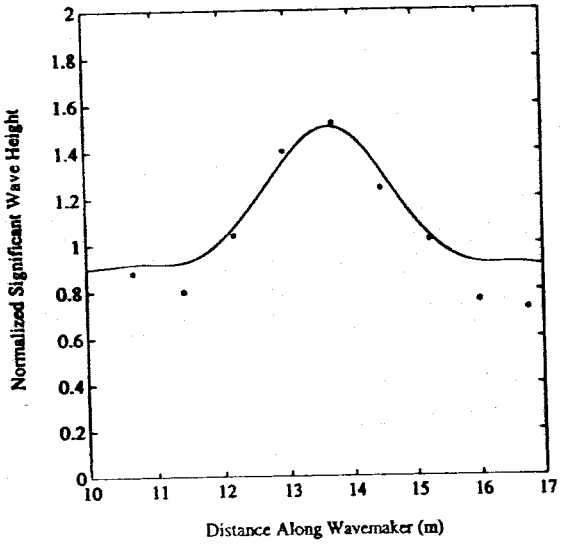

Figure 8: Case N4: Normalized Significant Wave Height at Transect at $x = 12.2$ m

Results for Case B4 are presented in Figures 9 and 10. These results also confirm that the effect of the breaking term cannot be seen in these cases without breaking.

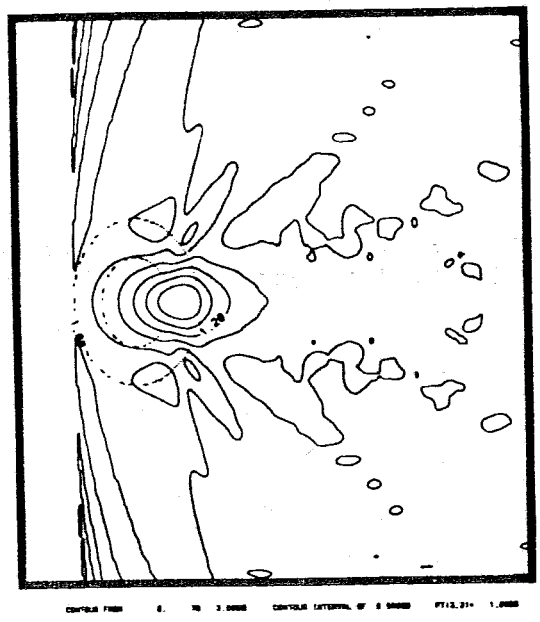

Figure 9: Case B4: Contour Plot of Normalized Significant Wave Height

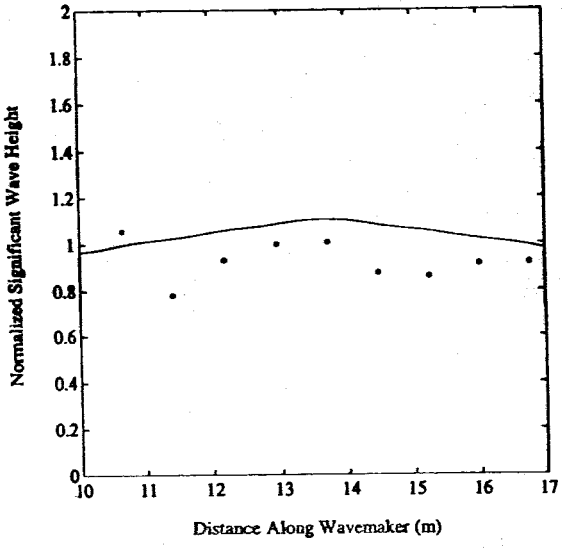

Figure 10: Case B4: Normalized Significant Wave Height at Transect at $x = 12.2$ m

Breaking Cases

The next two cases involve breaking waves and are denoted as Cases N5 and B5. Case N5 involves a narrow frequency spectrum as well as a narrow directional distribution, whereas Case B5 involves a broad frequency spectrum and a broad direction distribution. Details about the values of the free parameters for these cases can be obtained from Vincent and Briggs (1989).

Results for Case N5 are presented in Figures 11 and 12, where the first of these shows a contour plot of the computed normalized significant wave height and the second shows a comparison of model and data at Transect 4.

It can be seen that the experimental wave height shows a tendency to decrease around $y = 14$ m; the model does not predict this behavior. It is also seen that the data show a tendency to recover the initial significant wave height at $y = 10$ m and $y = 17$ m, whereas the model does not show this tendency.

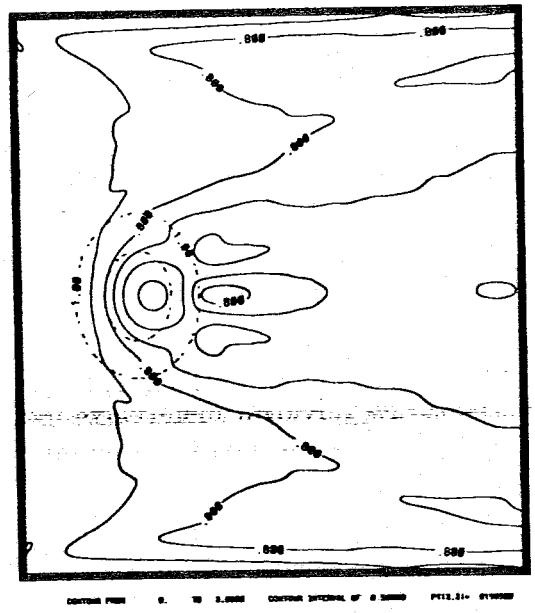

Figure 11: Case N5: Contour Plot of Normalized Significant Wave Height

Results for Case B5 are presented in Figures 13 and 14. Figure 14 shows that the model is predicting a fairly constant wave height, but the data show a decrease in the midsection.

Conclusions

Computed results involving cases without wave breaking agree well with laboratory data by Vincent and Briggs (1989). This demonstrates that the coefficient of the breaking term stays small in cases where wave breaking does not occur. The model also accurately predicts the shoaling and decay of statistical wave height for unidirectional random wave propagation onto a beach. However, the model does not accurately predict the shoaling and decay of the wave height for a multidirectional random sea. This behavior might be linked to the fact that no modifications have been made to the energy dissipation model to account for directional effects. Pronounced nonlinear effects may also have to be modeled more completely.

Özkan

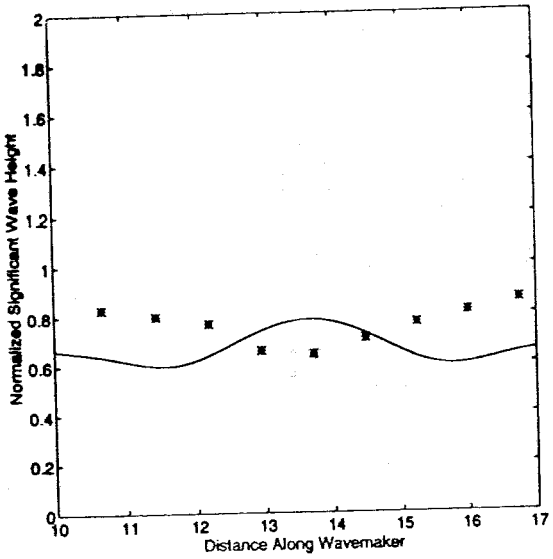

Figure 12: Case N5: Normalized Significant Wave Height at Transect at $x = 12.2$ m

In order to address these problems we need a more complete understanding of the physical processes causing the behavior observed in the two cases involving breaking waves in Vincent and Briggs' (1989) experiment. For this reason, an experiment involving waves on a submerged shoal has been designed with the intention of concentrating on directional effects on the energy dissipation and on nonlinear effects during breaking. The speed of the breaking waves will be observed and similarities to the speed of a bore will be investigated. The experiment is currently in progress and it is anticipated that the collected data will aid in the further development of the model.

Acknowledgement

This research has been sponsored by the U.S. Army Corps of Engineers, Coastal Engineering Research Center (Contract No. DACW 39-90-D-0006-D002) and by NOAA Office of Sea Grant, Department of Commerce, under Grant No. NA/6RG0162-01 (Project No. R/OE-9). The U.S. Government is authorized to produce and distribute reprints for governmental purposes, not withstanding any copyright notation that may appear hereon.

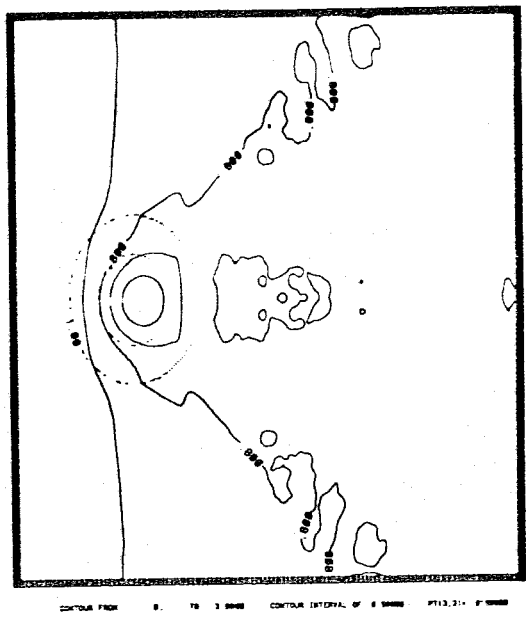

Figure 13: Case B5: Contour Plot of Normalized Significant Wave Height

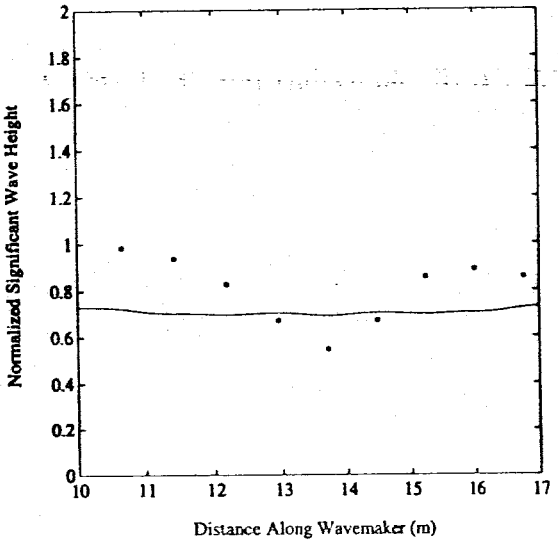

Figure 14: Case B5: Normalized Significant Wave Height at Transect at $x = 12.2$ m

References

Berkhoff, J. C. W., 1972, "Computation of combined refraction-diffraction", *Proc. 13th Intl. Conf, Coast. Engineering*, Vancouver, 471-490.

Booij, N., 1981, " Gravity Waves on Water with Non-uniform Depth and Current", Reprt No. 81-1, *Communication on Hydraulics*, Department of Civil Engineering, Delft University of Technology.

Borgman, L. E., 1985, "Directional spectrum estimation for the S_{xy} gauges," *Technical Report*, Coast. Engrg. Res. Center, Waterways Experiment Station, Vicksburg, MS, 1-104.

Grassa, J. M., 1990, "Directional random waves propagation on beaches", *Proc. 22nd Intl. Conf. Coastal Engrng.*, Delft, 798-811.

Hedges, T.S., 1976, "An empirical modification to linear wave theory," *Proc. Inst. Civ. Eng.*, 61, 575-579.

Hughes, S. A., 1984, "The TMA shallow-water spectrum description and applications," *Technical Report*, Coast. Engrg. Res. Center, Waterways Experiment Station, Vicksburg, MS.

Kirby, J.T., 1986, "Higher-order approximations in the parabolic equation method for water waves", *J. Geophys. Res.*, 91, 933-952.

Kirby, J. T. and Dalrymple, R. A., 1984, "Verification of a parabolic equation for propagation of weakly nonlinear waves", *Coastal Engrng.* 8, 219-232.

Kirby, J. T. and Dalrymple, R. A., 1986, "An approximate model for nonlinear dispersion in monochromatic wave propagation models", *Coast. Eng.*, **9**, 545-561.

Kirby, J. T. and Dalrymple, R. A., 1992, "REF/DIF S Version 1.0, Documentation and User's Manual", CACR 92-06, Coast. Engrg. Res Center, Waterways Experiment Station, Vicksburg, Miss

Mase, H. and Kirby, J.T., 1992, "Modified frequency-domain KdV equation for random wave shoaling," *Proc. Intl. Conf. Coast. Engrg.*, Venice.

O'Reilly, W. C. and Guza, R. T., 1991, "Comparison of spectral refraction and refraction-diffraction wave models", *J. Waterway, Port, Coastal and Ocean Engrng.*, 117, 199-215.

Panchang, V. G., Pearce, B. R., Wei, G. and Cushman-Roisin, B., 1990, "Solution of the mild-slope wave problem by iteration", *Applied Ocean Res.*, 13, 187-199.

Thornton, E. B. and Guza, R. T., 1983, "Transformation of wave height distribution", *J. Geophys. Res.*, 88, 5925-5938.

Vincent, C. L. and Briggs, M. J., 1989, "Refraction and diffraction of irregular waves over a mound", *J. of Waterway, Port, Coastal, and Ocean Engineering*, 115, 269-284.

Özkan